J Pharmacol Sci **112**, 373 – 377 (2010)

Journal of Pharmacological Sciences

Short Communication

Cellular Ca^{2+} Dynamics in Urinary Bladder Smooth Muscle From Transgenic Mice Overexpressing Na^+-Ca^{2+} Exchanger

Hidemichi Murata[1], Shingo Hotta[1], Eiji Sawada[1], Hisao Yamamura[1], Susumu Ohya[1], Satomi Kita[2], Takahiro Iwamoto[2], and Yuji Imaizumi[1,*]

[1]*Department of Molecular and Cellular Pharmacology, Graduate School of Pharmaceutical Sciences, Nagoya City University, Nagoya 467-8603, Japan*
[2]*Department of Pharmacology, School of Medicine, Fukuoka University, Fukuoka 814-0180, Japan*

Received November 17, 2009; Accepted January 5, 2010

Abstract. The rise of Ca^{2+} concentration ($[Ca^{2+}]_i$) by reducing external Na^+ in urinary bladder smooth muscle cells (UBSMCs) from transgenic mice overexpressing Na^+/Ca^{2+} exchanger type-1.3 (NCX1.3$^{tg/tg}$) was about 4 times as large as that in the wild-type (WT). NCX1 protein expression in UB increased about 4-fold in NCX1.3$^{tg/tg}$. The Ca^{2+} release by caffeine in UBSMCs was comparable between NCX1.3$^{tg/tg}$ and WT, but $[Ca^{2+}]_i$ decay was faster in NCX1.3$^{tg/tg}$. Contractions induced by acetylcholine, 60 mM K^+, or electrical stimulation were significantly smaller in UB segments of NCX1.3$^{tg/tg}$. NCX worked in Ca^{2+}-extrusion mode during these contractions in UBSMCs of both WT and NCX1.3$^{tg/tg}$.

Keywords: Na^+-Ca^{2+} exchanger, urinary bladder smooth muscle, transgenic mouse

The Na^+/Ca^{2+} exchanger (NCX) is a bidirectional antiporter and transports three Na^+ per Ca^{2+} in an electrogenic manner in cardiac myocytes (1). NCX is an essential molecule for extruding Ca^{2+} from the cytosol following the influx through voltage-dependent L type Ca^{2+} channels (VDCCs) and the Ca^{2+}-induced Ca^{2+} release (CICR) from sarcoplasmic reticulum (SR) during the excitation–contraction coupling and, thus, to maintain the physiological regulation of intracellular Ca^{2+} ($[Ca^{2+}]_i$) dynamics in cardiac myocytes (2). The Ca^{2+} influx via the reverse mode of NCX occurs in cardiac myocytes only under limited conditions, where the transmembrane Na^+ gradient is reduced and the membrane is depolarized (1, 2). However, its functional roles in smooth muscle (SM) appear to be more complicated, since both modes have been supposed to work under physiological conditions in different preparations (3 – 5). The most probable reason why functional roles of NCX in SM cells (SMCs) is so equivocal may be the much lower expression of the molecule in these cells compared to that in cardiac myocytes. The transgenic mice, which specifically overexpress NCX1.3 in SMCs (NCX1.3$^{tg/tg}$), have been introduced to shed light on this problem from a new direction (6). Under resting conditions in vascular SMCs, NCX has been suggested to function in the reverse mode and the related salt-sensitive hypertension was found in NCX1.3$^{tg/tg}$ (6). The present study was undertaken to elucidate the contribution of NCX to Ca^{2+} dynamics and contractility of urinary bladder SMCs (UBSMCs) by comparing NCX1.3$^{tg/tg}$ and wild-type (WT) mice.

NCX1.3$^{tg/tg}$ and WT male mice, 8 – 10-week-old, were used. Generation of the mice overexpressing NCX1.3 specifically in SMCs has been reported previously (6). All experiments were carried out according to the guiding principles for the care and use of laboratory animals (the Science and International Affairs Bureau of the Japanese Ministry of Education, Culture, Sports, Science, and Technology) and also with the approval of the ethics committee at Nagoya City University.

Single SMCs were enzymatically isolated from UB (7). Fura-2 fluorescent signals were measured by the ARGUS/HiSCA imaging system (Hamamatsu Photonics, Hamamatsu) at 23 ± 2°C (8). The isometric measurements of contractility were carried out as reported previously (7). Real-time quantitative PCR was performed by using Syber Green chemistry on an ABI 7000 sequence detector (Applied Biosystems, Foster City, CA, USA) as described previously (9). The following PCR primers

*Corresponding author. yimaizum@phar.nagoya-cu.ac.jp
Published online in J-STAGE on February 20, 2010 (in advance)
doi: 10.1254/jphs.09319SC

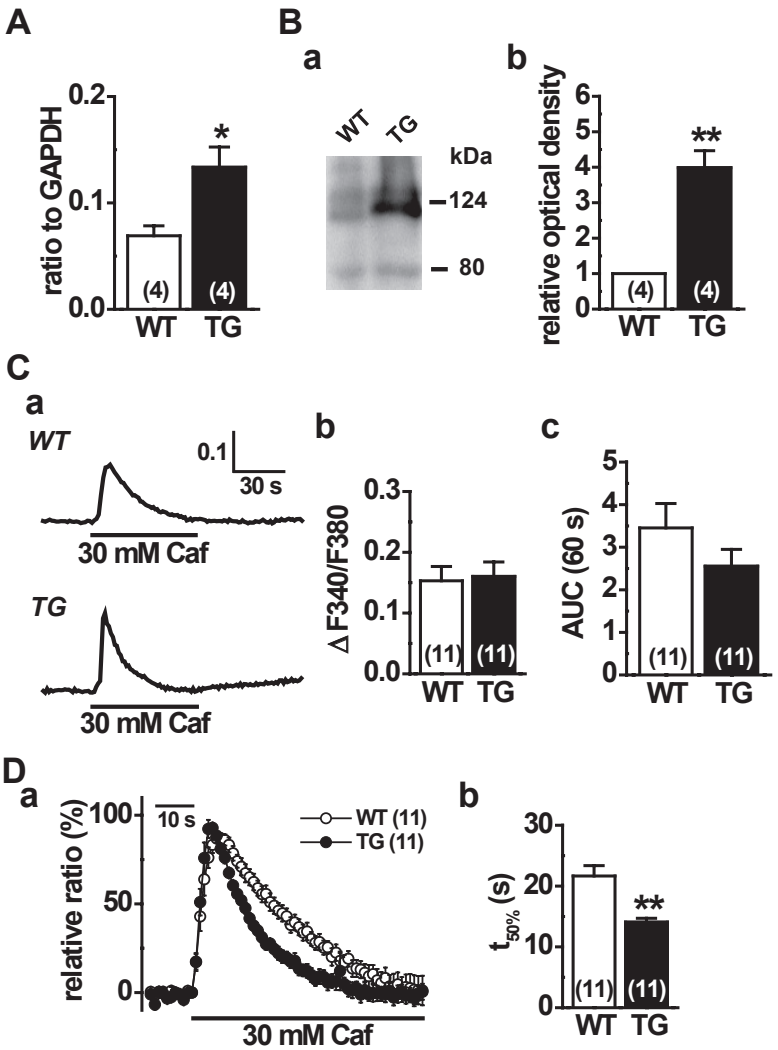

Fig. 1. NCX1.3 expression and Ca^{2+} dynamics induced by caffeine. A: Expression of NCX1 mRNA in UB from WT and NCX1.3$^{tg/tg}$ was examined by quantitative PCR and shown as the ratio relative to that of GAPDH. The number of experiments is shown in parentheses. B: Expression of NCX1.3 protein from UB of NCX1.3$^{tg/tg}$ was examined by Western blotting. Summarized results were obtained as the optical density of the band corresponding to NCX1 in UB from NCX1.3$^{tg/tg}$ relative to that in WT (b). C: $[Ca^{2+}]_i$ rise elicited by application of 30 mM caffeine (Caf) was monitored by the *F340/F380* ratio of the fura-2 signal in the whole cell area of UBSMCs from WT and NCX1.3$^{tg/tg}$. The summarized data show the peak *ΔF340/F380* (b) and the integrated area between the resting *F340/F380* level and *F340/F380* signal during the application of caffeine for 60 s (c). D: The time course of *ΔF340/F380* during the application of caffeine was averaged after each record was normalized at the peak. The duration of *ΔF340/F380* change during caffeine application was measured at the half maximum of the peak ($t_{50\%}$). In A, B, and D, $*P < 0.05$ and $**P < 0.01$: statistically significant difference between two groups.

were used for real-time PCR analysis: NCX1 2300 – 2434, 135 bp (GenBank accession no. AF004666). Western blotting analysis was performed in the same manner as described previously (8).

Direct electrical stimulation (ES) was performed in the presence of 1 μM atropine, 1 μM phentolamine, 1 μM propranolol, 1 μM tetrodotoxin, and 10 μM suramine. Standard Krebs solution contained 112 mM NaCl, 4.7 mM KCl, 2.2 mM $CaCl_2$, 1.2 mM $MgCl_2$, 25 mM $NaHCO_3$, 1.2 mM KH_2PO_4, 14 mM glucose (pH 7.4 with 95% O_2 – 5% CO_2 at 36°C). High K^+ solution was prepared by replacing NaCl with equimolar KCl. HEPES-buffered Krebs solution having the following composition was used for $[Ca^{2+}]_i$ measurements 120 mM NaCl, 4.8 mM KCl, 1.2 mM $CaCl_2$, 1.3 mM $MgSO_4$, 5.8 mM glucose, 10 mM HEPES, 1.2 mM KH_2PO_4, and 12.6 mM $NaHCO_3$ and pH was adjusted to 7.4 with NaOH. Zero Na^+ solution was prepared by the equimolar substitution of NaCl and $NaHCO_3$ with *N*-methyl-D-glucamine in HEPES-buffered Krebs solution and pH was adjusted to 7.4 by HCl. Data are expressed as the mean ± S.E.M. in the text. Statistical significance between two groups was examined by Student's *t*-test after the *F*-test: $*P < 0.05$, $**P < 0.01$.

Figure 1A summarizes the results from quantitative analyses of NCX1 mRNA in UB from WT and NCX1.3$^{tg/tg}$ mice. The expression of NCX1 transcripts relative to that of GAPDH in NCX$^{tg/tg}$ was significantly larger than that in WT. The expression of NCX1 protein in UB was also examined with Western blotting (Fig. 1B: a and b). The expression level in UB of NCX1.3$^{tg/tg}$ was approximately 4 times as high as that in WT ($P < 0.01$).

In single UBSMCs loaded with fura2-AM, the resting *F340/F380* was comparable between WT and NCX1.3$^{tg/tg}$ (0.352 ± 0.014, n = 32; 0.362 ± 0.017, n = 30, $P > 0.05$). The application of 30 mM caffeine induced transient rise of $[Ca^{2+}]_i$, which was monitored by *F340/F380* (Fig. 1Ca). The *F340/F380* reached the peak within 10 s from

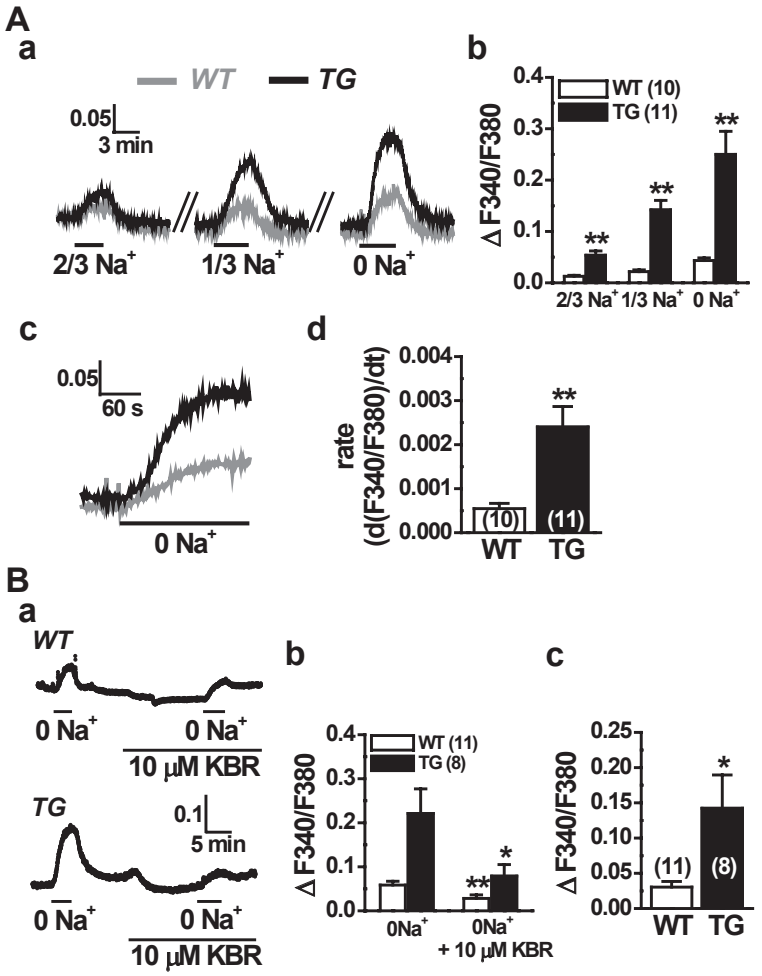

Fig. 2. $[Ca^{2+}]_i$ rise due to NCX in reverse mode by exposure to low Na^+ solution. A: Changes in $[Ca^{2+}]_i$ by the decrease in Na^+ concentration in the external solution from 137 to 91 (2/3), 46 (1/3), and 0 mM were recorded in UBSMCs in WT (gray lines) and NCX1.3$^{tg/tg}$ (black lines) (a). The summarized data show averaged *ΔF340/F380* under these conditions (b). The rising phase of *F340/F380* change following the solution exchange to 0 Na^+ was demonstrated in faster time scale in c. The rate of rise in *ΔF340/F380* is summarized in d. $^{**}P < 0.01$: statistically significant difference between two groups. B: Effects of 10 μM KB-R7943 (KBR) on the $[Ca^{2+}]_i$ rise due to the exchange to 0 Na^+ were recorded in a. The data of *ΔF340/F380* in the absence and presence of 10 μM KBR are summarized in b. $^{*}P < 0.05$ and $^{**}P < 0.01$: statistically significance difference in the absence and presence of KBR in each group. The KBR-sensitive components of *ΔF340/F380* are shown in c. $^{*}P < 0.05$: statistically significant difference between two groups.

the start of caffeine application. The peak of *ΔF340/F380* and the integrated area of *F340/F380* from the resting level (AUC) for 60 s in the response to caffeine in NCX1.3$^{tg/tg}$ were not significantly different from those in WT, respectively (Fig. 1C: b and c). In contrast, the decline of *F340/F380* from the peak to the resting level in NCX1.3$^{tg/tg}$ was apparently faster than that in WT (Fig. 1Ca). When the peak *ΔF340/F380* was normalized as 100% in each record, it was apparent that the decline in NCX1.3$^{tg/tg}$ was faster than that in WT. The duration of *F340/F380* rise at the half maximum of each peak ($t_{50\%}$) in NCX1.3$^{tg/tg}$ was approximately 65% of that in WT ($P < 0.01$) (Fig. 1Db).

When the concentration of Na^+ ($[Na^+]_o$) in the bathing solution was reduced to two thirds (2/3 Na^+: 91 mM), one third (1/3 Na^+: 46 mM), or zero (0 Na^+), the rise of $[Ca^{2+}]_i$ was detected in a manner depending on the decrease in $[Na^+]_o$ (Fig. 2Aa). The original records and summarized data indicate that *ΔF340/F380* induced by 0 Na^+ in NCX1.3$^{tg/tg}$ was approximately 5.8 times as large as that in WT ($P < 0.01$) (Fig. 2Ab). The rising phase of *ΔF340/F380* following the reduction of $[Na^+]_o$ to 0 is shown in Fig. 2Ac and the rate of rise is summarized in Fig. 2Ad. The rate of rise in NCX1.3$^{tg/tg}$ was approximately 4.4 times as large as that in WT ($P < 0.01$).

The $[Ca^{2+}]_i$ rise induced by 0 Na^+ was challenged with 10 μM KB-R7943, an inhibitor of NCX (10) (KBR in Fig. 2B). The *ΔF340/F380* was significantly decreased by KB-R7943 in both groups ($P < 0.05$, respectively) but the decrease was more prominent in NCX1.3$^{tg/tg}$ than in WT. In the presence of KBR, the *ΔF340/F380* by 0 Na^+ was not significantly different between the two groups ($P > 0.05$) (Fig. 2Bb). The KBR-sensitive component of *ΔF340/F380* in NCX1.3$^{tg/tg}$ was significantly larger than that in WT ($P < 0.05$) (Fig. 2Bc).

The contractile responses to 10 μM acetylcholine (ACh) (Fig. 3A), 60 mM K^+ solution (Fig. 3B) and ES (Fig. 3C) were measured in tissue segments of UB. The peak amplitude of contractions induced by these stimuli in NCX1.3$^{tg/tg}$ was significantly smaller than those in WT, respectively ($P < 0.01$ in ACh and ES and $P < 0.05$ in 60 mM K^+). The AUCs of contractions for 10 min

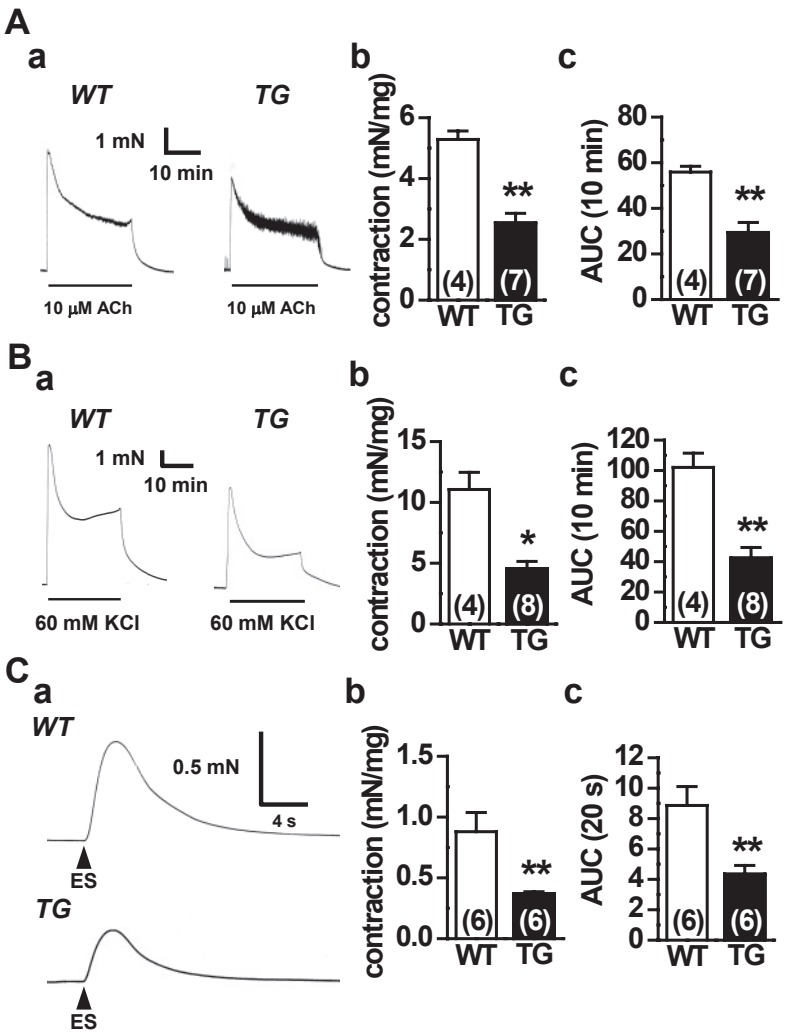

Fig. 3. Contractions induced by ACh, high K^+, and ES in UB segments from WT and NCX1.3$^{tg/tg}$. A: Typical recordings of isometric tension development due to 10 μM ACh in UB segments is demonstrated in a. Data for the peak amplitude of contraction and integrated area of contraction above the resting tension for 10 min are summarized in b and c, respectively. In b, the peak amplitude of contraction was divided by the tissue weight in each preparation (mN/mg), throughout A – C. B: Typical recordings of isometric tension development due to 60 mM K^+ and summarized data of the peak amplitude and the integrated area for 10 min are shown in a, b, and c, respectively. C: Typical recordings of twitch contraction due to ES and summarized data of the peak amplitude and the integrated area are shown in a, b, and c, respectively. Twitch contractions were elicited by a train of 10 pulses (3 ms in duration, 300 mA in strength, 200 ms in interval, once every 90 s) in the presence of 1 μM atropine, 1 μM phentolamine, 1 μM propranolol, 1 μM tetrodotoxin, and 10 μM suramine. In A, B and C, $*P < 0.05$ and $**P < 0.01$: statistically significant difference between two groups.

during the responses to ACh and 60 mM K^+ and that of twitch contraction by ES in NCX1.3$^{tg/tg}$ were also significantly smaller than those in WT, respectively ($P < 0.01$).

NCX1 protein expression in UB increased approximately 4-fold in NCX1.3$^{tg/tg}$ in comparison with that in WT. The finding that the KB-R7943–sensitive component of *ΔF340/F380* induced by 0 Na^+ also increased approximately 4-fold in NCX1.3$^{tg/tg}$ is consistent with the extent of protein overexpression. In contrast, the $t_{50\%}$ of caffeine-induced $[Ca^{2+}]_i$ transients in UBSMCs from NCX1.3$^{tg/tg}$ was 65% of that in WT, suggesting 1.5 times faster half-sequestration of Ca^{2+} from the cytosol. Since Ca^{2+} uptake into SR and mitochondria may also contribute to the Ca^{2+} sequestration, the 1.5 times faster $t_{50\%}$ in NCX1.3$^{tg/tg}$ may be reasonable with respect to 4 times overexpression of NCX protein. These results indicate that overexpressed NCX1.3 significantly facilitated membrane Ca^{2+} transport in either direction, acting in both forward and reverse modes in UBSMCs.

It has been reported that overexpression of NCX1 in cardiac myocytes of the mice results in changes in SR Ca^{2+} contents, as well as $[Ca^{2+}]_i$ transients (11). In UBSMCs, SR Ca^{2+} content was not significantly changed in NCX1.3$^{tg/tg}$ in the standard external solution. On the other hand, the peak amplitude of contraction in UB segments from NCX1.3$^{tg/tg}$ was significantly smaller than that in WT, when segments were challenged with three different stimuli: ACh, 60 mM K^+, or ES. These stimuli provide $[Ca^{2+}]_i$ elevation by combination of separate signal pathways: i) Ca^{2+} release from SR via formation of IP_3, ii) Ca^{2+} influx through VDCC, and iii) Ca^{2+} release from SR via CICR through ryanodine receptors (8). The decreased contractile responses in NCX1.3$^{tg/tg}$ may be due to significantly potentiated Ca^{2+} extrusion from the cytosol by overexpressed NCX. It has been, however, shown that the contractile response to U46619, a thromboxane A_2 analogue, in aortic tissue from NCX1.3$^{tg/tg}$ is

not significantly different from that in WT (12). The reason for the dissociated results is not clear in this study, but it may possibly be due to the difference in cellular excitability, which is much higher in UBSMCs than in aortic SMCs. Entered Ca^{2+} through VDCC may be more preferentially extruded by NCX located nearby.

The Ca^{2+} transport by NCX in the reverse mode has been reported in vascular smooth muscle under the conditions where $[Na^+]_i$ is elevated by treatment with ouabain (6). The findings suggesting that NCX functions in the reverse mode under physiological conditions have been accumulating (13, 14). Under pathophysiological conditions, the up-regulation of NCX and its accelerated functions in reverse mode has been also reported (6, 15). The possible roles of NCX in reverse mode in UBSMCs under physiological and pathophysiological conditions remain to be carefully examined using $NCX1.3^{tg/tg}$.

Acknowledgments

This work was supported by a Grant-in-Aid for Scientific Research on Priority Areas (20056027) from the Japanese Ministry of Education, Culture, Sports, Science, and Technology and by a Grant-in-Aid for Scientific Research (B) (20390027) from the Japan Society for the Promotion of Science to YI.

References

1 Shigekawa M, Iwamoto T. Cardiac Na^+-Ca^{2+} exchange. Molecular and pharmacological aspects. Circ Res. 2001;88:864–876.
2 Bers DM. Cardiac excitation-contraction coupling. Nature. 2002; 415:198–205.
3 Ashida T, Blaustein MP. Regulation of cell calcium and contractility in mammalian arterial smooth muscle: the role of sodium-calcium exchange. J Physiol. 1987;392:617–635.
4 Bradley KN, Flynn ER, Muir TC, McCarron JG. Ca^{2+} regulation in guinea-pig colonic smooth muscle: the role of the Na^+-Ca^{2+} exchanger and the sarcoplasmic reticulum. J Physiol. 2002;538: 465–482.
5 Rebolledo A, Speroni F, Raingo J, Salemme SV, Tanzi F, Munin V, et al. The Na^+/Ca^{2+} exchanger is active and working in the reverse mode in human umbilical artery smooth muscle cells. Biochem Biophys Res Commun. 2006;339:840–845.
6 Iwamoto T, Kita S, Zhang J, Blaustein MP, Arai Y, Yoshida S, et al. Salt-sensitive hypertension is triggered by Ca^{2+} entry via Na^+/Ca^{2+} exchanger type-1 in vascular smooth muscle. Nat Med. 2004;11:1193–1199.
7 Hotta S, Morimura K, Ohya S, Muraki K, Takeshima H, Imaizumi Y. Ryanodine receptor type 2 deficiency changes excitation-contraction coupling and membrane potential in urinary bladder smooth muscle. J Physiol. 2007;582:489–506.
8 Yamazaki D, Aoyama M, Ohya S, Muraki K, Asai K, Imaizumi Y. Novel functions of small conductance Ca^{2+}-activated K^+ channel in enhanced cell proliferation by ATP in brain endothelial cells. J Biol Chem. 2006;281:38430–38439.
9 Ohya S, Kimura K, Niwa S, Ohno A, Kojima Y, Sasaki S, et al. Malignancy grade-dependent expression of K^+-channel subtypes in human prostate cancer. J Pharmacol Sci. 2009;109:148–151.
10 Kimura J, Watano T, Kawahara M, Sakai E, Yatabe J. Direction-independent block of bi-directional Na^+/Ca^{2+} exchange current by KB-R7943 in guinea-pig cardiac myocytes. Br J Pharmacol. 1999;128:969–974.
11 Wang J, Chan TO, Zhang XQ, Gao E, Song J, Koch WJ, et al. Induced overexpression of Na^+/Ca^{2+} exchanger transgene: altered myocyte contractility, $[Ca^{2+}]_i$ transients, SR Ca^{2+} contents, and action potential duration. Am J Physiol Heart Circ Physiol. 2009; 297:H590–H601.
12 Karashima E, Nishimura J, Iwamoto T, Hirano K, Hirano M, Kita S, et al. Involvement of Na^+-Ca^{2+} exchanger in cAMP-mediated relaxation in mice aorta: evaluation using transgenic mice. Br J Pharmacol. 2007;150:434–444.
13 Besarani D, Wu C, Fry CH. The influence of changes in extracellular and intracellular sodium concentration on detrusor contractility. BJU Int. 2006;97:1083–1086.
14 Hirota S, Janssen LJ. Store-refilling involves both L-type calcium channels and reverse-mode sodium-calcium exchange in airway smooth muscle. Eur Respir J. 2007;30:269–278.
15 Zhang S, Dong H, Rubin LJ, Yuan JX. Upregulation of Na^+/Ca^{2+} exchanger contributes to the enhanced Ca^{2+} entry in pulmonary artery smooth muscle cells from patients with idiopathic pulmonary arterial hypertension. Am J Physiol Cell Physiol. 2007;292: C2297–C2305.